INDIAN JOURNAL OF SCIENCE AND TECHNOLOGY

Corresponding author.

bakkialakshmis@rocketmail.com

Investigating the Effect of the Azo Dye Amaranth on Beta Lactoglobulin by Multi-Spectroscopic Techniques and Molecular Docking: Role in Protein Aggregation

S Gayathri[1], S Bakkialakshmi[2]*

1 Research scholar, Department of Physics, Annamalai University, Tamil Nadu, India
2 Professor, Department of Physics, Annamalai University, Tamil Nadu, India

Abstract

Objectives: This study explored the interaction mechanism between the synthetic azo dye amaranth (AMA) and the widely consumed whey protein beta-lactoglobulin (BLG), using multi-spectroscopic techniques combined with a molecular docking study. Neurodegenerative diseases are often marked by protein aggregation; hence, this study examined the effect of AMA-induced aggregation on BLG at low pH. **Methods:** The interaction mechanism was investigated at physiological pH using UV–Vis absorption, steady-state and time-resolved fluorescence, Fourier transform infrared (FTIR) spectroscopy, Forster's theory of non-radiation energy transfer, and molecular docking techniques. Biophysical studies, such as turbidity, circular dichroism spectra, and FESEM analysis, have been used to characterize AMA-induced aggregation in BLG. **Findings**: Steady-state fluorescence quenching of BLG by AMA revealed that the quenching process was dominantly static, owing to complex formation. This was confirmed using time-resolved fluorescence data. BLG showed one binding site for the AMA dye, with a binding affinity of 10^5 mol/L. According to the FRET analysis, the estimated distance between the binding of BLG and AMA was 3.24 nm. Conformational changes in the BLG were revealed through synchronous fluorescence and FTIR spectroscopy as a result of AMA interaction. Molecular docking studies have suggested that AMA predominantly binds to BLG via hydrogen and hydrophobic bonds. The results of the turbidity experiments showed that AMA concentration affected BLG aggregation. Changes in BLG secondary structure were detected by circular dichroism spectra. FESEM measurements confirmed the amyloid-like structure of the aggregated BLG. **Novelty**: The experimental results of turbidity analysis revealed that even at low concentrations (0.8 mM) and room temperature, the interaction between the azo dye AMA and BLG can cause protein misfolding, leading to the formation of amyloid aggregates. This research aims to study the harmful effects of edible azo dyes and their ability to initiate the formation

of amyloid aggregates linked to various neurodegenerative disorders.

Keywords: Amaranth; Betalactoglobulin; Fluorescence quenching; Docking; Amyloid aggregation

1 Introduction

The color of food can influence consumer choices and food quality. Many popular foods, such as jellies, milk products, and treats, use artificial food colors made from chemicals derived from coal tar that contain azo groups. Synthetic dyes are used instead of natural dyes because they are more stable under light and pH, dissolve easily in water, have low contamination rates, and are cheaper to produce. It is important to note that some foods and beverages have a high amount of artificial coloring, including some that are prohibited. Studies have reported that synthetic food coloring, such as yellow 5 (tartrazine), red 40 (Allura red), and Food yellow 3 (sunset yellow), may contain carcinogenic contaminants and cause health problems, including allergies and hyperactivity disorder in children[1].

Amaranth is a synthetic mono-azo dye, also known as trisodium(4E)-3-oxo-4-[(sulfonate-1-naphthyl) hydrazono] naphthalene-2,7-disulfonate, and is widely used to visually enhance the appearance of various food and drink products, including beverages, wines, sauces for salads, coffee, candies, caviar, and cake batter[2]. According to the FAO and WHO Food Additives Expert Committee, the recommended daily intake of this substance should not exceed 0.5 mg/kg. This dye has the potential to cause health issues like allergic reactions, asthma (due to histamine production), or hives. However, there are concerns that they may cause hyperactivity and may contain cancer-causing residues. Additionally, it induces the formation of calcareous deposits in the kidneys[3].

Cow milk is composed of various proteins, and beta-lactoglobulin (BLG) is the major protein, accounting for 50-60% of the total protein content. BLG is made up of 162 amino acids and has a molecular weight of 18.4 kDa. BLG has a flattened beta-barrel structure with eight anti-parallel beta-strands, allowing it to bind both hydrophilic and hydrophobic chemicals. It is rich in cysteine, which is essential for the synthesis of glutathione, an anticarcinogenic tripeptide. BLG is commonly found in beverages and foods that promote muscle growth and overall health[4]. It is known for its ability to bind strongly to hydrophobic molecules through its hydrophobic core and interior cavity. BLG can also bind to ligands through non-covalent interactions like electrostatic and hydrogen bonding. Additionally, it is widely used as a model protein for studying protein folding and aggregation. Protein aggregation is a crucial process in various biological phenomena and has significant implications for medical and technological applications. Proteins have a high tendency to form aggregates *in vitro*[5].

Protein aggregates, known as amyloid assemblies, have been linked to several debilitating human disorders, including Alzheimer's, Parkinson's, and type II diabetes. The presence of protein aggregates is a common characteristic of both diseases. Under acidic pH, various proteins such as human serum albumin, myoglobin, and lysozyme tend to form amyloid aggregates[6–8]. Protein aggregation is essential in several aspects and its implications in medicine and technology are far-reaching. Some azo dyes like Allura red, quinone yellow, and sunset yellow have been found to interact with proteins and induce protein aggregation[6,8,9], which can have significant implications for various biological and biomedical processes. Amaranth may pose health risks, including its accumulation in the plasma and its interaction with human serum albumin, which can alter its secondary structure[10,11]. In a study conducted by Li et al., it was found that hydrophobic forces play a role in the formation of the complex between AMA and alpha-lactalbumin and amaranth has an impact on the conformation and functionality of alpha-lactalbumin, leading to modifications in its secondary structure[12].

Investigating the interaction between the dye and milk protein is crucial for understanding the transportation and metabolism of AMA dyes at the molecular level. This study used various multi-spectroscopic methods, such as UV-Vis absorption, fluorescence, FRET, and computational analysis to understand the molecular mechanism of AMA dye binding to BLG. The study observed that the interaction between the dye and milk protein leads to a change in the molecular conformation of milk protein, which could affect its physiological function. Fluorescence measurements were used to investigate the mode of interaction and its mechanism, whereas synchronous fluorescence and FTIR measurements were used to monitor conformational changes and secondary structure modifications induced by AMA on BLG. To identify the precise binding site involved in the interaction between AMA and BLG, a molecular docking analysis was conducted. This interaction is of great significance in the fields of chemistry, life science, and clinical medicine. This study provides insights into how negatively charged amaranth interacts with protonated BLG and the resulting aggregation at acidic pH values. The study utilized Turbidity and FESEM analyses to investigate the effect of AMA on BLG aggregation, and the aggregates' secondary structure was calculated using Far UV-CD spectroscopy. This study is the first of its kind to examine AMA-induced amyloid fibrillation of BLG proteins. The primary objective of this study was to comprehensively analyze the biological characteristics of food dyes, with a focus on food safety. The research outcomes are expected to facilitate the acquisition of further information on the toxic properties of AMA dye by the scientific community.

2 Methodology

2.1 Reagents and chemicals

Beta Lactoglobulin (purity $\geq$ 90%), Amaranth (Dye content, 85-95%) & 1.0 M phosphate buffer solution (PBS) (7.4) were procured from Sigma Aldrich Company, Bangalore. All reagents used were of analytical grade, and phosphate buffer and distilled water were used as the solvents.

2.2 Stock solution preparation

To prepare a solution of 1×10^{-5} M BLG stock (0.02 mg/ml)), 1 M phosphate buffer (at physiological pH 7.4) was utilized. The concentration of BLG was measured using a spectrophotometer with an extinction coefficient of 11,000 $M^{-1}cm^{-1}$ at 282 nm. 1×10^{-4} M AMA dye (6.04 mg/ml) was dissolved in distilled water. Both protein and dye stock solutions were made freshly.

2.3 UV-Visible spectroscopic analysis

A UV-visible spectrophotometer (Shimadzu, UV 1800) was used to perform the absorption measurements. The prepared solutions' spectra were recorded in the range of 200-800 nm using a quartz cell with a 1 cm optical path length.

2.4 Steady-state and synchronous fluorescence spectroscopy

A Shimadzu RF-5301PC spectrofluorometer was used to obtain steady-state and synchronous fluorescence spectra. Steady-state fluorescence spectra of beta-lactoglobulin were recorded at varying AMA concentrations using intrinsic fluorescence spectroscopy. The emission wavelength ranged from 250 to 500 nm and the excitation wavelength was 282 nm. Both the excitation and emission slit widths were maintained at 5.0 nm. To remove the inner filter and reabsorption, $F_C = F_{ob}e^{\frac{A_{ex}+A_{em}}{2}}$, was used to correct the fluorescence data. (F_{ob}), the measured fluorescence intensity, and the corrected fluorescence intensity (F_c), respectively. The absorption of the dye at the excitation and emission wavelengths is represented by the symbols A_{ex} and A_{em}, respectively. Synchronous fluorescence spectra of the BLG protein were recorded at the same AMA concentration used for fluorescence measurements. Fixed $\Delta\lambda$ values of 15 nm and 60 nm evaluated the changes in the microenvironment of tyrosine and tryptophan residues in biomolecules.

2.5 Time-resolved fluorescence measurements

Fluorescence lifetime intensity decay was measured with a Fluorolog - FL3-11 spectrofluorometer, using a time-correlated single photon counting method and a nano-LED source (Jobin Yvon) as an excitation source. The fitting of the decays was based on the residual function and the χ^2 value.

2.6 FTIR measurements

FTIR spectra of BLG and BLG-AMA samples in the range from 4000 to 1200 cm^{-1} with a resolution of 4.0 cm^{-1} were recorded using a Perkin Elmer spectrometer. The FTIR acquisition used ethanol instead of H_2O to minimize solvent interference.

2.7 Molecular docking

The Auto Dock 1.5.6 software downloaded from the SWISS-MODEL Repository was used to perform molecular docking of AMA to BLG (http://autodock.scripps.edu/). The 3D coordinates of the BLG docking simulation were obtained using the X-ray crystal structure (PDB ID: 3NPO) available at 2.20 Å in the RCSB database. The protein X-ray crystal structure was refined by removing unnecessary water molecules and optimizing polar hydrogen atoms. Auto Dock was used to assign the Kollman charges. A grid box measuring 82 × 74× 68 Å was created, encompassing the entire active site cavity of the BLG, with a grid spacing of 0.375 as the default. The two-dimensional crystal structure of AMA (CID: 13507) was downloaded from the National Center of Biological Information (PubChem database). Amaranth was docked flexibly by merging nonpolar hydrogens, imposing Gasteiger charges, counting aromatic carbons and rotatable bonds, determining the TORSDOF, and converting it into the PDBQT format. (Protein Data Bank, Partial Charge (Q), and Atom Type (T)) file format using Auto Dock Tools version 1.5.6. Flexible ligand-protein docking was performed using the Lamarckian Genetic Algorithm (LGA). The BLG was kept rigid and the input torsion roots of the flexible AMA ligand were established. The study involved 10 genetic algorithm (GA) runs, with parameters including a population size of 150, a maximum of 2.5 million energy evaluations, and a maximum of 27,000 generations. All other parameters were set to their default values. The stable conformation of the docked complexes with the lowest binding energy was determined and the best-docked poses were visualized using PyMol and BIOVIA Discovery Studio.

2.8 Turbidity measurements

UV-visible spectrophotometer Shimadzu-UV 1800 was utilized to measure turbidity levels and analyze the aggregation of BLG induced by AMA by taking absorbance at 650 nm. 0.1 mM BLG (0.2 mg/ml) was dissolved in 10 ml of glycine-HCl buffer at pH 2.0. Different concentrations of AMA (0.0 to 2.0 mM) were treated with 0.2 ml of BLG. The samples were incubated overnight at room temperature. Turbidity levels were measured in samples that only contained AMA at pH 2.0.

2.9 Circular Dichroism (CD)

A J-815 (150S) Circular Dichroism Spectrometer was used to measure how BLG's secondary structure of BLG changed in response to the AMA dye. At pH 2.0, BLG (0.2 mg/mL) was subjected to various AMA dye doses (0.4 mM, 0.6 mM, and 1.2 mM). To get rid of extra free dye, the AMA-treated BLG samples were centrifuged for 20 min at 3500 rpm before the CD tests. To prevent noise in CD readings, centrifugation was carried out. To perform far-UV CD measurements, 400 μL of the AMA-treated BLG samples were filled into a quartz cuvette with a path length of 1 mm. At room temperature, the spectra were recorded in the 200–250 nm range, with a spectral bandwidth of 2 nm and scanning speed of 100 nm min^{-1}.

2.10 Field Emission Scanning Electron Microscope (FESEM)

A CARL ZEISS-SIGMA 300 FESEM examined the surface morphology of the BLG aggregates. Fifty microliters of the sample containing BLG (0.2 ml) treated with amaranth (1.8 mM) was incubated overnight at pH 2.0 and applied on the surface of the conductive carbon tape on the aluminum stub, followed by air-drying at ambient temperature for 24 h. Subsequently, a thin layer of chromium was sputter-coated onto the surfaces of the samples under vacuum. The chromium-coated samples were placed on the FESEM with an operating voltage of 0.02-20 KV, and images were captured.

3 Results

3.1 Absorption spectral study

UV−Vis is an exploratory and convenient technique to investigate the binding interaction of the Protein–ligand molecules. During titration, changes in UV-vis spectra, such as hypochromic/hyperchromic effects and/or hypsochromic/bathochromic shifts, can indicate interactions between ligands and proteins. Figure 1 shows the UV-Vis absorption spectra of BLG with different concentrations of AMA. The absorption spectra of BLG without and with AMA were obtained by subtracting the AMA-free form from the BLG-AMA system. Figure 1(b) shows similar concentrations of amaranth dye without protein (BLG)

as the control. In Figure 1 (a) the initial spectrum represents the fixed concentration (0.2×10^{-5} M) of free BLG (control) without Amaranth which exhibits maximal absorbance at 282 nm due to the π-π^{*} transitions of aromatic amino acids (tryptophan and tyrosine) residues. The absorption of BLG at 282 nm steadily increased with increasing AMA concentration, which is a result of the formation of a complex between BLG and AMA. This complex exposes the Trp and Tyr residues to the external environment, which is favorable for the π-π^{*} transition of Trp and Tyr residues[13]. A significant change was observed in the absorption maxima of beta-lactoglobulin (BLG), leading to a 5 nm shift towards the blue end of the spectrum. A shift in λ_{max} indicates a change in polarity near the tryptophan residue, leading to modification of the peptide strand of beta-lactoglobulin (BLG) molecules[14]. As a result, the molecule's hydrophobicity changed, indicating that amaranth could bind to BLG.
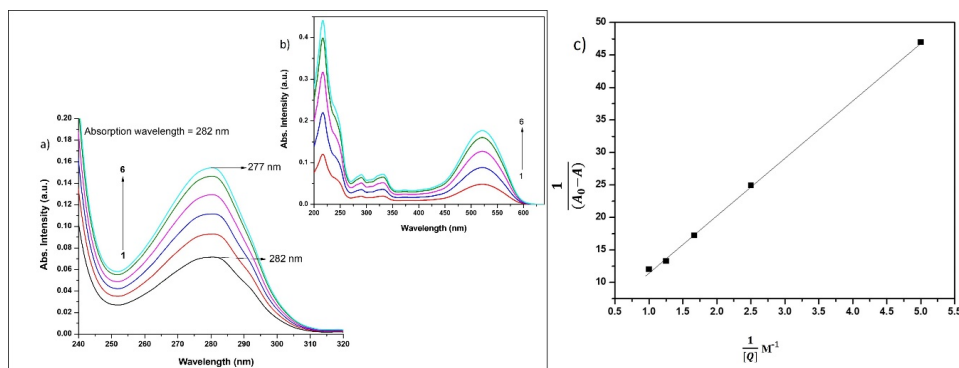
Fig 1. (a) UV$-$Vis absorption spectra of beta-lactoglobulin with different concentrations of amaranth (1) 0.0, (2) 0.2, (3) 0.4, (4) 0.6, (5) 0.8, and (6) 1.0×10^{-4} M,(b) Absorption spectra of amaranth (1) 0.2, (2) 0.4, (3) 0.6, (4) 0.8, and (5) 1.0×10^{-4} M, c) plot of $\frac{1}{A_{0-A}}$ versus $\frac{1}{[Q]}$ for BLG with AMA

A plot was created between $1/(A_0\text{-}A)$ and $1/[Q]$ (Figure 1(c)), where A_0 and A represent the absorbance of the unbound protein (BLG) and AMA-BLG complexes, respectively. Measurements were taken at 282 nm with different AMA concentrations, where [Q] corresponds to the molar concentration of AMA. Based on the linear plot, it can be concluded that there is 1:1 complexation in the BLG-AMA system[11]. The binding constant K_b was calculated to be 2.9×10^4 L mol^{-1} at pH 7.4 (298 K) by dividing the intercept by the slope (Figure 1 (c)). The linear regression coefficient $R^2 = 0.99$.

3.2 Fluorescence Quenching Mechanism and Binding Parameters

Fluorescence quenching is a physiochemical process used to evaluate the nature of interactions between protein-ligand complexes. Quenching can occur through various mechanisms such as the formation of complexes, energy transfer, reactions in excited states, and collisional quenching. Proteins contain chromophoric groups on different amino acids, including phenylalanine, tyrosine, and tryptophan, which give rise to endogenous fluorescence. The maximum emission wavelength of these amino acids is dependent on the hydrophobicity of the surrounding microenvironment. BLG exhibits fluorescence owing to the presence of two tryptophan and four tyrosine residues[11]. These aromatic amino acids contribute to the fluorescence of the protein. Throughout the current study, the concentration of BLG remained constant at 0.2×10^{-5} M, while increasing concentrations of amaranth were used (ranging from 0 to 1.0×10^{-4} M). The fluorescence emission spectrum of BLG showed an emission maximum at 333 nm in its native state. Upon interaction with AMA, a slight blue shift of 2 nm was observed in the emission maximum (from 333 to 331 nm), along with a gradual decrease in the fluorescence intensity[15].

To investigate the quenching mechanism, the fluorescence intensity data were analyzed using the Stern-Volmer quenching equation.

$$\frac{F_0}{F} = 1 + K_q \tau_0 [Q] = 1 + K_{sv}[Q] \tag{1}$$

The equilibrium fluorescence emission intensities with and without the quencher (AMA) are represented by F and F_0, respectively, where $K_q = \frac{K_{sv}}{\tau_0}$. Several important factors must be considered when studying protein quenching. The Stern-Volmer constant, K_{SV}, is one such factor. Along with the quencher concentration [Q], the biomolecular quenching rate constant, K_q, and an average lifetime of the protein without any quencher, denoted as τ_0, can be calculated from time-resolved fluorescence measurements. To determine K_{sv}, the relative fluorescence intensity (F_0/F) was measured as a function of AMA concentration
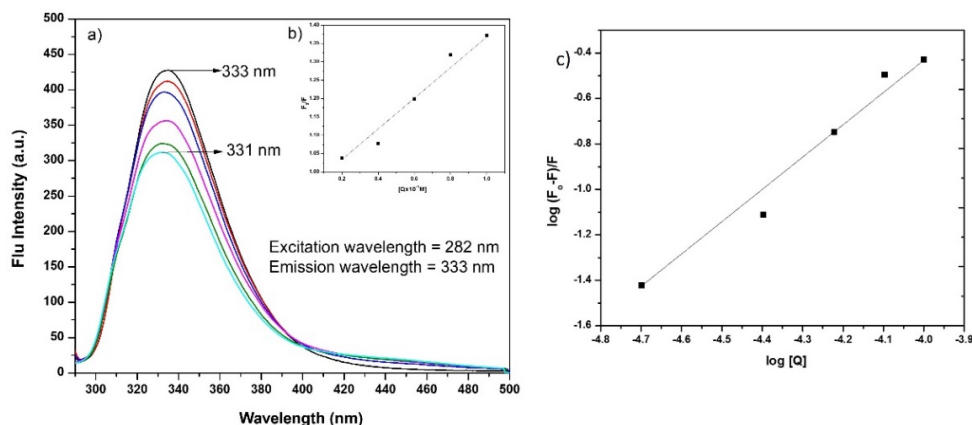
Fig 2. (a) Steady-state fluorescence spectra of beta-lactoglobulin with different concentrations of amaranth (1) 0.0, (2) 0.2, (3) 0.4, (4) 0.6, (5) 0.8 & (6) 1.0×10^{-4} M (b) The inset panel presents the Stern−Volmer plot for BLG with AMA (c) Double logarithmic plot of beta-lactoglobulin with amaranth

at 298 K. The slope of the linear function of F_0/F versus [Q] provides the necessary values for $K_{sv} = 4.55 \times 10^3$ L mol^{-1}. K_q is as high as 2.57×10^{12} M^{-1}s^{-1}.

For static quenching, small molecules independently bind to equivalent sites of a macromolecule, the binding constant (K_a) and number of binding sites (n) can be determined from the fluorescence data using the double logarithmic Equation (2) [16] was used to calculate the number of binding sites (n) and binding constant (K_a) of BLG-AMA complex

$$log \left[\frac{F_0 - F}{F} \right] = log k_a + n log[Q] \tag{2}$$

The double reciprocal plot (Figure 2(c)) produces a straight line with a high linear correlation coefficient (R^2=0.99). By analyzing the intercept and slope of the double-log plot, the values of K_a and n were found to be 4.69×10^5 L mol^{-1} and 1.3, for the BLG-AMA complex. Equation (3) allows for the calculation of the binding free energy [16].

$$\Delta G = -2.303 RT l_n K_a \tag{3}$$

The gas constant is represented by R, while the temperature is denoted by T (298 K). The BLG-AMA complex was analyzed and found to have a ΔG value of -74.46 KJ mol^{-1}, indicating negative free energy.

3.3 Synchronous Fluorescence Spectroscopy

Protein conformational changes were analyzed using synchronous fluorescence spectroscopy. This technique provides information regarding polarity changes in the chromophore microenvironment. The synchronous fluorescence spectrum shows a distinct peak for tryptophan residues at 60 nm. Similarly, the peak for tyrosine residues in proteins was observed at a wavelength of 15 nm. Alterations in the polarity of the surrounding environment can be determined by analyzing the change in peak emission. The synchronous fluorescence spectra of BLG and the complex after the addition of AMA are presented in Figure 3 **a** and **b**, respectively.

The fluorescence intensity of BLG decreased as the AMA concentration increased for both $\Delta \lambda = 15$ nm and 60 nm. The emission peak of tyrosine residues did not shift significantly with increasing amaranth concentrations. However, there was a slight blue shift at $\Delta \lambda = 60$ nm, indicating that Trp residues underwent conformational changes upon binding with AMA. These results suggest that AMA binding causes conformational changes in the BLG.

3.4 Time−resolved fluorescence study

Time-resolved fluorescence measurements were performed to determine the quenching mechanisms. Several factors, such as the environment surrounding the fluorophore, interactions in the excited state, relaxation induced by solvents, and conformations of proteins, can affect the lifetime of the excited state. It has been suggested through steady-state analysis that the observed fluorescence quenching may be attributed to the fluorescence energy transfer mechanism from BLG to AMA. Analysis
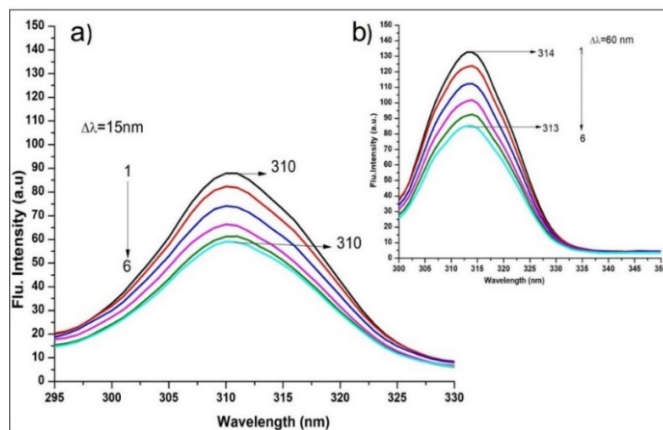
Fig 3. Synchronous fluorescence spectra of beta-lactoglobulin with amaranth at (a) Δl=15 nm and (b) Δl =60 nm

of the electronic spectra and Stern-Volmer indicated that a static quenching mechanism occurred during the interaction between BLG and AMA. It is generally known that dynamic quenching alters a fluorophore's excited state lifetime because quenching depopulates the excited state. In Figure 4, the exponential curve of the fluorescence decay of BLG as the AMA concentration increased is displayed. The fitted values are listed in Table 1. A triexponential decay was observed in the BLG-AMA system. In the BLG, Trp residues exhibit three distinct lifetimes. Two of these lifetimes are inherent to the Trp residues themselves (Trp 19 and Trp 61), regardless of the surrounding structural environment. The third lifetime is generated by the interaction between Trp residues and neighboring amino acids[17].

The BLG-AMA system utilizes three exponentials to precisely fit the decay curves and calculate the various lifetime components. The results showed that $\tau_1 = 0.93$ ns contributed 37.64% (α_1), $\tau_2 = 2.11$ ns contributed 59.74% (α_2), and $\tau_3 = 6.15$ ns contributed 2.62% (α_3) of the total fluorescence for pure BLG. Instead of focusing on the individual decay constants, the average lifetime was calculated using Equation (4).

$$< \tau > = \frac{\propto_1 \tau_1^2 + \propto_2 \tau_2^2 + \propto_3 \tau_3^2}{\alpha_1 \tau_1 + \alpha_2 \tau_2 + \alpha_3 \tau_3} \tag{4}$$
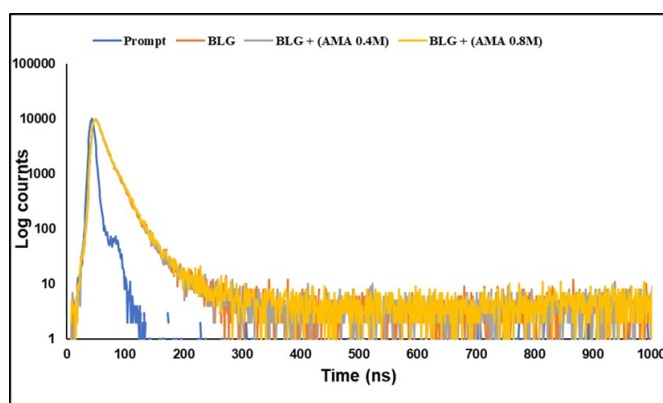
Fig 4. Time-resolved fluorescence decay of beta-lactoglobulin phosphate buffer (pH =7.4) with different concentrations of amaranth (1) 0.0, (2) 0.4, and (3) 0.8 × 10^-4 M

Based on the data presented in Table 1, it can be concluded that the average lifetime components of βLG, namely τ_1, τ_2, and τ_3, remained unaffected by the increase in the concentration of AMA. The quenching mechanisms of the interactions between amaranth and BLG were confirmed by lifetime measurements. This was further supported by data fitting, with a χ^2 ~1.00. Figure 4 shows that there was no observable distinction in the decay curves of BLG as the quantity of AMA increased. As shown in Table 1, the fluorescence lifetime (τ) of BLG was not affected by the azo dye.

Table 1. Fluorescence lifetime and relative amplitudes of BLG with different concentrations of AMA

Concentration (M)	Lifetime (ns)			Average lifetime x 10^{-9} sec	Relative amplitude			χ^2	S.D 10^{-11} sec		
	τ_1	τ_2	τ_3		α_1	α_2	α_3		τ_1	τ_2	τ_3
BLG	0.93	2.11	6.15	1.77	37.64	59.74	2.62	1.2	6.49	3.71	18.34
BLG+ AMA (0.4M)	0.86	2.04	6.1	1.74	36.9	59.84	3.26	1.39	5.48	3.91	11.84
BLG+AMA (0.8M)	0.84	2.04	7.14	1.73	35.47	62.29	2.23	1.72	4.4	2.77	11.84

3.5 Fluorescence resonance energy transfer (FRET) between AMA and BLG

Utilizing fluorescence resonance energy transfer (FRET), spectroscopy can accurately and non-invasively determine the distance between donor and acceptor molecules. The overlapping fluorescence spectra of BLG (donor) and UV–Vis absorption spectra of AMA (acceptor) are shown in Figure 5. The following equations determine the energy transfer efficiency (E) using Forster's non-radiative energy transfer theory:

$$E = 1 - \frac{F}{F_0} = \frac{R_0^6}{R_0^6 + r^6} \tag{5}$$

$$R_0^6 = 8.79 \times 10^{-25} \times k^2 N^{-4} \varphi J \tag{6}$$

$$J = \frac{\sum F(\lambda)\varepsilon(\lambda)\lambda^4\Delta\lambda}{\sum F(\lambda)\Delta\lambda} \tag{7}$$

Förster's hypothesis states that the efficiency of energy transfer (E) between a donor and an acceptor is determined by the distance (r) between them and a characteristic distance (R_0) known as the Förster radius, at which the transfer efficiency is 50%. In Equation (5) F and F_0 refer to the fluorescence intensities of the donor molecule with and without the acceptor molecule, respectively. The value of r represents the distance between acceptor and donor molecules. Additionally, the value of k^2 is a spatial orientation factor for the dipole and is equal to 2/3. This value is the average calculated over all possible angles. The medium's refractive index is denoted by N=1.336. The fluorescence quantum yield of the donor is represented by Φ =0.15. Meanwhile, the overlap integral of the donor's emission spectrum and the acceptor's absorption spectrum is represented by J, which can be calculated using Equation (7). The fluorescence intensity of the donor within a specific wavelength range from λ to $\lambda + \lambda$ is denoted as F(λ). On the other hand, the extinction coefficient of the acceptor at λ is represented as $\varepsilon(\lambda)$.
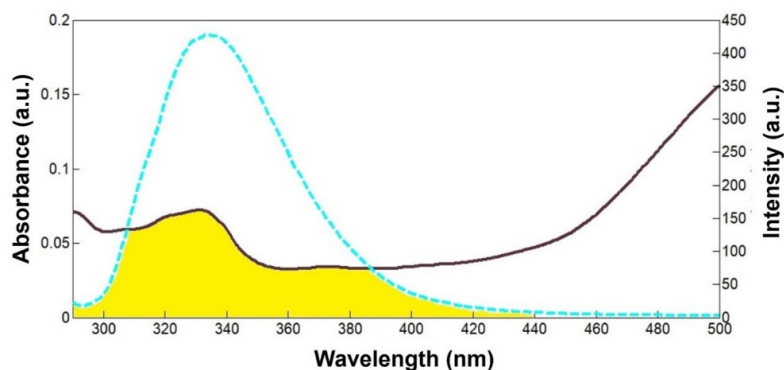
Fig 5. The overlap of UV absorption spectra of Amaranth (solid line) with the fluorescence emission spectra of Beta-lactoglobulin (dashed line)

In this instance, AMA acts as the acceptor, the tryptophan residue of the BLG protein serves as the donor, and the shaded area in Figure 5 delineates sufficient spectral overlap between the molecules. According to Equations (5), (6) and (7), the parameters were calculated such that J = 7.38× 10^{-15} cm^3 L M^{-1}, E = 0.34, R_0 = 2.91 nm, and the overlap distance r is 3.24 nm, which is less than 8 nm, the distance required for FRET to occur[14].

3.6 Effect of AMA binding on BLG secondary structure

FTIR spectroscopy was used to evaluate the impact of alterations in the protein's secondary structure upon interaction with small compounds. Figure 6 shows the representative infrared spectra of BLG and BLG+AMA in the 1200–4000 cm^{-1} range. Both native BLG and AMA+BLG showed similar infrared spectral patterns. Binding of BLG to AMA did not result in the emergence of any new spectral signals, indicating the absence of any new covalent bond formation during the binding process. The amide I band is a composite of C=O group vibrations in the polypeptide backbone, providing insight into the protein's secondary structure, ranging from 1700 to1600 cm-1[18], between 1610 and 1627 cm^{-1} depicted as intramolecular β-sheets, and between 1660 and 1699 cm^{-1} for β-turns. Because of this qualitative data, the amide I region has been extensively used for conformational studies of proteins. FTIR peak assignments of BLG have been extensively used for the conformational studies of proteins.
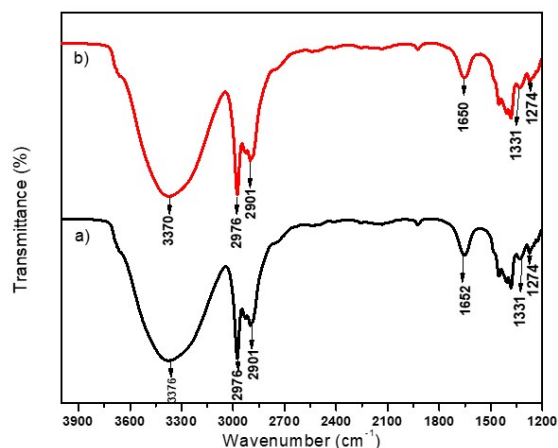
Fig 6. FTIR Spectra of a) Beta lactoglobulin, b) Beta-lactoglobulin + amaranth

The absorption bands at 1652 cm^{-1} (Figure 6a) in the BLG spectra correspond to the amide I vibration (C =O). After binding with AMA, as shown in Figure 6b, caused a shift in the amide I group band from 1652 cm^{-1} to 1650 cm^{-1}. The band has undergone a shift from 3376 to 3,370 cm^{-1} (Figure 6 a), which can be attributed to the N-H stretch. The bands observed at 2901 and 2976 cm^{-1} were primarily caused by the stretching of C-H bonds. The N-H bending and C-N stretching were responsible for the amide III bands that appeared between 1220 and 1330 cm^{-1}. These results indicate a change in the secondary protein structure during BLG-AMA interactions[14].

3.7 Molecular Docking

In silico docking predicts the optimal orientation of the ligand (AMA) in the receptor's active site and investigates the compatibility between a ligand and a protein (BLG) target at the molecular level. Beta-lactoglobulin, a protein composed of a single polypeptide chain comprising 162 amino acid residues, is a prime example of a protein that can be analyzed using in silico docking. The essential part of the beta-lactoglobulin structure is composed of an α-helix and nine anti-parallel β-strands. These strands form a cone-shaped barrel composed of eight β-sheets, which creates a hydrophobic pocket. The β-strand A–H form of the β-barrel is the central calyx of the BLG crystal structure, and it is the primary binding site of many ligands, especially palmitic acid. The primary binding site was named site 1, located in the internal cavity of the β-barrel, whereas site 2 was identified to be toward the exterior of the β-barrel. These are the two most likely binding sites in BLG. Molecular docking was performed using AMA at BLG's primary binding site of BLG. The findings are displayed in Figure 7. The AMA appeared to fit comfortably in the hydrophobic cavity of the BLG.

As shown in Figure 7b six hydrogen bonds were found to stabilize the AMA-BLG complex, with Glu62 (2.68 Å), Ser116(1.95 Å), Lys69 (1.89 Å, and 1.78 Å), Asn88 (1.65 Å and 2.93 Å), and Asn109(2.27 Å) residues, and one carbon-hydrogen bond with Lys60 (2.83 Å). Further stabilizing the BLG-AMA complex were two hydrophobic contacts with Pi-Alkyl Leu39 (5.05 Å) and Pi-Alkyl Val41 (5.11 Å). These bindings may be disturbed in a highly protonated environment such as at pH 2.0. The best conformation had an inhibition constant of 1.18 μM and total intermolecular energy of -13.27 cal/mol. The Van der Waals, Hbond+ desolvation, and electrostatic energies were -10.77 kcal/mol, -10.23 kcal/mol, and -0.54 kcal/mol, respectively. The

docking results showed that amaranth had good docking scores with BLG, with binding energy of -8.09 Kcal/mol. The more negative the value, the better is the binding free energy between the receptor BLG and the ligand AMA[19].
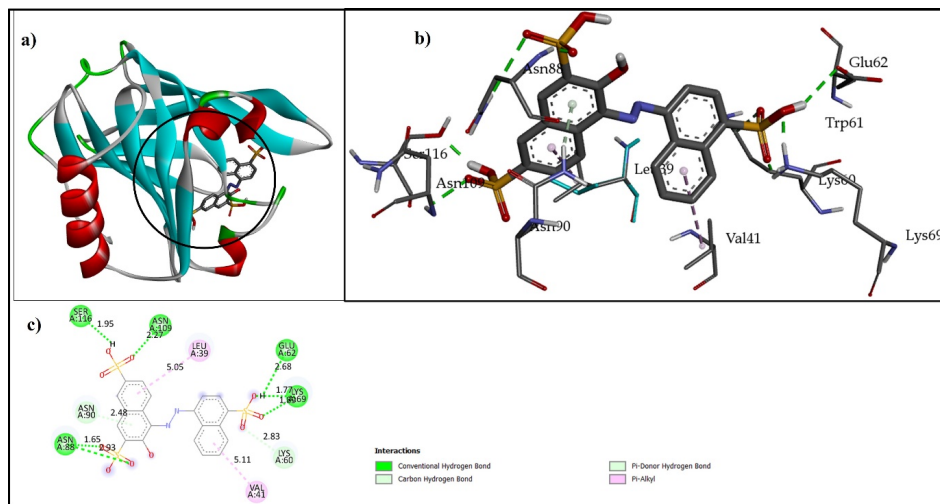
Fig 7. (a) 3D molecular docking, (b) 3D ligand interaction, and (c) 2D diagram ligand interaction of BLG with the AMA dye

3.8 Protein aggregation studies

3.8.1 Turbidity measurements

Turbidity, as a protein aggregation indicator, was quantified with the addition of increasing amounts of amaranth concentration (0.0 to 2.0 mM). The turbidity of BLG with and without AMA was measured at pH 2 (Figure 8). Turbidity was measured above 600 nm because AMA absorbance was almost zero at this wavelength[20].

It was evident from Figure 8, that beta-lactoglobulin at pH 2.0, without amaranth, did not show any turbidity, indicating that BLG itself does not form aggregates upon pH reduction. The turbidity was initiated at a concentration of 0.2 mM, after which the turbidity value increased drastically and reached a maximum at 0.8 mM concentration, after which the plateau remained constant till 2.0 mM concentration of AMA. From these results, it can be noted that the minimal concentration of AMA required to induce aggregation in BLG is 0.2mM. This showed that the control samples (pure BLG and pure Amaranth (without the addition of either BLG or AMA) dye at pH 2) do not show any turbidity, which confirms that the Amaranth itself does not aggregate and turbidity arises when BLG aggregates in the presence of Amaranth. The turbidity profile of BLG does not show a sigmoidal curve, that is it does not have a lag phase[21].
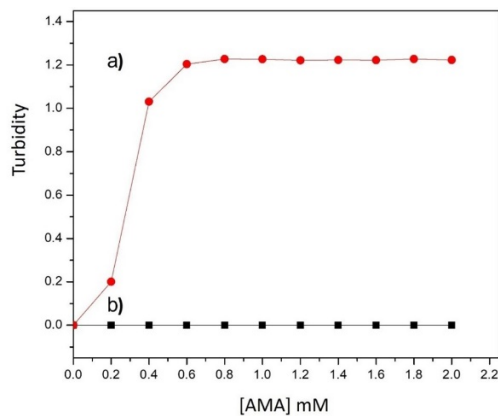
Fig 8. Turbidity profile (a) Beta-lactoglobulin versus amaranth dye (pH 2.0) (b) amaranth alone (without the addition of BLG pH2.0)

3.8.2 FESEM analysis

To confirm the presence of the AMA-induced BLG fibrillar protein aggregates, representative FESEM images of the samples were obtained (Figure 9).
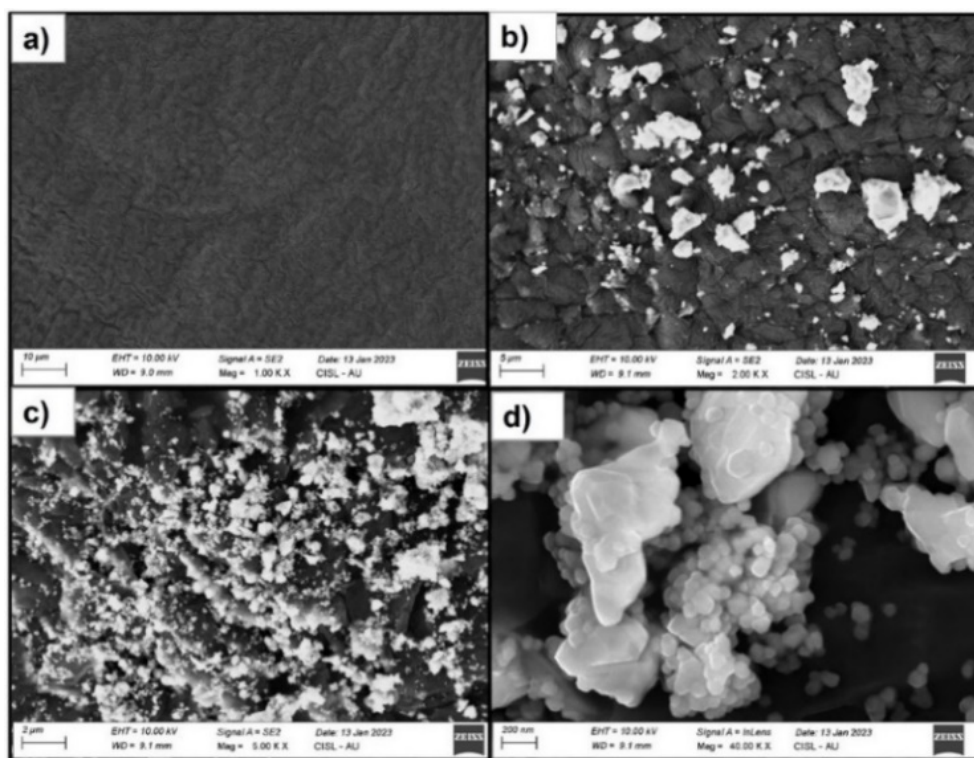
Fig 9. (a) BLG (0.2 mg ml^{-1}) without amaranth. (b) BLG (0.2 mg ml^{-1}) treated with 1.8 mM amaranth at pH 2. overnight incubation at 2.00KX magnification, (c) 5.00 KX magnification , and (d) 40.00 KX magnification

FESEM was used to detect AMA-induced aggregates in the BLG. FESEM images of BLG were obtained after incubation at pH 2.0, with and without 1.8 mM AMA, at room temperature (Figure 9**a**, **b**, and **c**). From the FESEM observations, BLG without AMA did not show any visible aggregate structure, as shown in Figure 10**a**, indicating that HGG did not undergo self-aggregation, which is correlated with the above spectroscopic result, and the formation of amorphous aggregates was observed for BLG+ AMA (Figure 9 **b, c** & **d**).

3.8.3 Circular Dichroism Studies

CD spectroscopy is often utilized to study changes in proteins' secondary structure. This technique helps in studying the modification of protein's secondary and tertiary structures by binding it with small molecules, as well as perturbing the structures of proteins. At pH 2.0, the secondary structure changes of BLG with and without AMA were examined through measurements of far-UV CD spectra. As shown in Figure 10 the far-UV CD spectra of BLG at pH 2.0 with low concentrations of AMA (0.0-1.6 mM) and without it displayed characteristic minima (210-222 nm) with low ellipticity, which could be attributed to the alteration of α-helical structure to other secondary structures such as β-sheet and random coil, which are typical hallmarks of protein aggregation[5,9]. Moreover, the presence of AMA at different concentrations also led to a decrease in the ellipticity of the BLG spectra. Table 2 indicates the percentage of secondary structural changes in BLG in response to the AMA dye. Specifically, the α-helix component decreased significantly from 15.23% to 3.26%, whereas the β-turn component increased from 33.23 % to 43.64%.
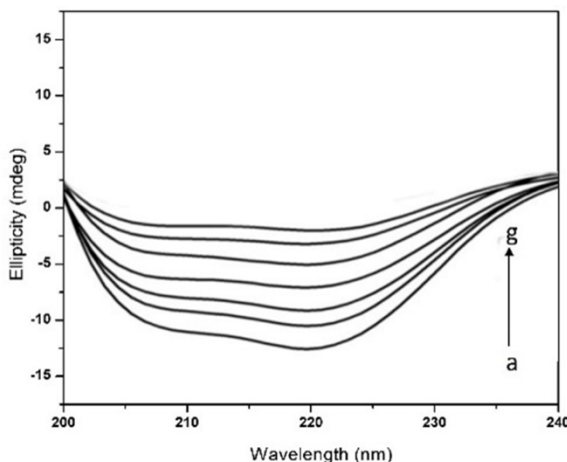
Fig 10. Far UV CD spectra of BLG (0.2 mM) in the presence of a) 0.0, b) 0.2, c) 0.4, d) 0.6, e) 0.8, f) 1.0, g) 1.2 of AMA

Table 2. The percent of α-helix and β-sheet content of BLG were calculated by the K2D2 software at different concentrations of amaranth

Concentrations	% α-Helix	% β-Sheet
BLG + 0.0 mM AMA	15.23	33.23
BLG + 0.2 mM AMA	13.32	35.69
BLG + 0.4 mM AMA	10.27	36.08
BLG + 0.6 Mm AMA	8.71	36.85
BLG + 0.8 mM AMA	6.34	39.23
BLG + 1.0 mM AMA	5.79	40.44
BLG + 1.2 mM AMA	4.34	41.24
BLG + 1.4 Mm AMA	3.26	43.64

4 Discussion

The objective of this study was to investigate how the azo-dye amaranth interacts with the whey protein beta-lactoglobulin through a combination of multi-spectroscopic and molecular docking studies. Additionally, this study provides empirical support for the aggregation of BLG stimulated by AMA dye at low pH levels. The study of UV-vis absorption shows that there is an increase in absorbance intensity and a significant shift towards shorter wavelengths on the absorption maxima of BLG due to the binding interaction with AMA (Figure 1). This binding can lead to changes in the microenvironment of aromatic amino acid residues. This suggests that AMA modifies the structure of BLG and leads to the formation of a BLG-AMA complex. In analogous research, the interaction between the whey protein alpha-lactalbumin and the artificial coloring agent quinone-yellow exhibited commensurate outcomes [22].

Fluorescence spectrum analysis of BLG revealed that the peak fluorescence emission was observed at 333 nm. However, upon the addition of AMA to the BLG solution, the intrinsic fluorescence of BLG was significantly reduced. Additionally, the emission maxima of BLG showed a blue shift of 2 nm, owing to the presence of AMA (Figure 2**a**). This indicates that AMA could bind to the chromophores of the protein, which are located in a hydrophobic cleft. As a result, the hydrophobic environment became more pronounced, causing water molecules to be displaced from the hydrophobic binding domain upon the addition of AMA. This finding is supported by similar results reported in the literature [15]. Protein (BLG) loses its fluorescence in the presence of a quencher (AMA), which can be caused by either a dynamic or static process of quenching. The majority of dynamic fluorescence quenching occurs because of intermolecular collisions between the quencher and the protein. It is important to

note that dynamic fluorescence quenching does not require actual binding of the ligand, so there is no change in the protein's conformation or function. When a stable protein-quencher complex is formed, it leads to static fluorescence quenching. The graphical representation of the Stern-Volmer equation shows a linear relationship for the BLG-AMA system (Figure 2 **b**). This indicated the presence of a single quenching mechanism in this system under steady-state fluorescence conditions.

The rate constant for quenching (K_q) in the BLG-AMA complex was much higher than the limiting dynamic diffusion rate constant (approximately $1 \times 10^{10} M^{-1}s^{-1}$) for various quenchers with biomolecules. K_q is as high as 2.57×10^{12} $M^{-1}s^{-1}$. These results suggest that the quenching mechanism of the BLG-AMA complex is initiated by static quenching, which is caused by the formation of a ground-state complex between BLG-AMA, rather than by dynamic collision. A recent study found a similar quenching mechanism when anthraquinones interacts with beta lactoglobulin [16]. The binding constant K_a and binding site values of and n were found to be 4.69×10^5 L mol^{-1} and 1.3, respectively, from the double logarithmic plot (Figure 2**c**). The n value suggests that there is a one-to-one interaction in the binding site of BLG, the binding constant values are on the order of 10^5 M^{-1}, and there is a strong binding affinity in the BLG-AMA complex [11] **.**

To validate the fluorescence outcomes, synchronous fluorescence spectra were conducted. AMA did not shift tyrosine's emission peak significantly. However, Trp residues undergo conformational changes with a slight blue shift at $\Delta\lambda$ = 60 nm upon binding with AMA (Figure 3), resulting in a shift from hydrophilic to hydrophobic in the microenvironment surrounding the residue, leading to folding of the peptide chain and loss of its ordered structure to form a new conformation. This suggests that AMA binding primarily affects the microenvironment polarity near Trp residues, with a minimal impact on the conformation near Tyr residues. To gain a deeper understanding of BLG's fluorescence mechanism of BLG towards AMA, the time-resolved fluorescence technique was utilized. During complex formation, the fluorescence lifetime of the fluorophore remained undisturbed, indicating that the quenching mechanism of BLG by amaranth is static quenching (Table 1). These findings confirm the results obtained through steady-state fluorescence spectroscopy and demonstrate that a ground-state complex was formed between AMA and BLG. The results showed a correlation with those reported in the literature that has been reported [11]. FRET functions as a molecular ruler to measure the overlap region; in this case, the overlap distance 'r' of the BLG-AMA complex was 3.24 nm (Figure 5). Salim et al. reported an overlap distance of 1.48 nm between fluvoxamine and human serum albumin, which also satisfies the 8 nm requirement and results from ground-state complexation between the two binding species [14]. This study revealed that there is a high chance of energy transfer via static quenching between BLG and AMA, with $0.5R_0 < r < 1.5R_0$, where R_0 signifies the Förster distance. Additionally, the study indicated a significant energy transfer between the BLG trp residues and AMA dye.

In the FTIR spectra (Figure 6), the C=O stretching vibration of the amide carbonyl group in the amide I band of BLG shifted from 1652 cm^{-1} to 1650 cm^{-1}. The spectral bands observed in the amide I region around 1660-1650 cm^{-1} were identified as originating from the alpha-helical structure of the protein. [23]. This shift in the amide I band to lower wave numbers is probably due to the interaction between BLG and amaranth, but it may also be due to a conformational change in BLG caused by local destabilization of the alpha-helix into loops. The band shifted from 3376 to 3,370 cm^{-1} (Figure 6**a**), which can be attributed to N–H stretching. These results confirm that the AMA-protein complexes cause polypeptide carbonyl hydrogen bonding network rearrangement [14]. These results indicate a change in the secondary protein structure during the BLG-AMA interaction.

The interaction between BLG and AMA was analyzed in detail using theoretical calculations through molecular docking, providing an atomic-level view of the complex (Figure 7). The docking results showed that amaranth had good docking scores with BLG, with binding energy of -8.09 Kcal/mol. Trp 61 residue is near the binding site of the ligand with BLG (Figure 7**a**); hence, computational results confirm the fluorescence study outcomes. Hydrophobic interactions and hydrogen bonds have both been implicated in the binding of ligands to the hydrophobic cavities of BLG in this study and have been well correlated with previously reported literature [15]. The BLG-amaranth interaction also involved charged residues, such as Lys60, Glu62, and Lys69, as well as polar amino acid residues, such as Asn88 and Asn109.

According to turbidity measurements, amaranth caused aggregation of BLG at a pH of 2. Aggregation kinetics typically follow sigmoidal curves with an initial lag phase, a growth phase, and an equilibrium phase. If protein aggregation pathways exhibit such curves, it indicates they are nucleus-dependent [21]. In this study, the lag phase was not present in the amaranth-induced aggregation (Figure 8), and BLG was directly converted into larger aggregates. The isoelectric point of BLG was reported to (pI) 5.34 [24]. Below the isoelectric point (<pI), the protein is positively charged and can interact electrostatically with negatively ionized substances in the solution. Amaranth consists of negatively charged sulfonic functional groups that interact with protonated amino acid residues (arginine, histidine, lysine) of BLG, causing amyloid aggregation. Hence, in the presence of 0.2-2.0 mM, AMA interacts electrostatically with protonated amino acids and neutralizes charges on BLG, causing aggregation. At low pH, charge neutralization perturbed the interaction between BLG and the solvent, promoting the formation of hydrophobic moieties that facilitate BLG aggregation. At low pH, charge neutralization perturbed the interaction between BLG and the solvent, promoting the formation of hydrophobic moieties that facilitate BLG aggregation. The aggregation induced

by AMA may have been influenced by both electrostatic and hydrophobic interactions[5].

Several scientific studies have provided evidence that beta-lactoglobulin (BLG) is capable of forming particulate structures when it reaches its isoelectric point[25]. Additionally, under conditions where the net charge on the polypeptide is higher, BLG can form amyloid fibrils. In the acidic environment of the gastric juice, BLG undergoes ionization and changes into a cationic form. This cationic form can then bind to the amaranth dye, resulting in the formation of amyloid protein clusters. This process is of significant interest to researchers exploring the potential health effects of BLG and its interactions with other molecules in the gastrointestinal tract.

Circular dichroism (CD) was employed to examine the secondary structures of beta-lactoglobulin (BLG) during aggregation. The decrease in the percentage of alpha-helices indicated the formation of beta-sheets or disordered conformations due to BLG aggregation in the solution (Figure 10). This phenomenon is commonly observed during fibril formation or aggregation of various proteins. Consequently, the helical stability of BLG was significantly reduced and the protein conformation unfolded owing to the addition of AMA[5,9].

BLG in an unfolded conformation exposes the hydrophobic surface that interacts with the AMA dye, forming disordered amorphous aggregates, as observed through FESEM analysis (Figure 9). A similar morphology of amorphous aggregates was induced in BLG when it interacted with sunset yellow dye, was reported in the literature[9]. Recent studies have linked the formation of protein aggregates with the onset of misfolding diseases, including Alzheimer's and Parkinson's diseases. Based on the available evidence, it can be inferred that amaranth has the potential to induce amorphous aggregation of beta-lactoglobulin. In denaturing conditions, short amyloid-like sheet stretches can be arranged randomly and closely, resulting in observed spherical particles (Figure 9**d**)

5 Conclusion

Using multi-spectroscopic studies and molecular docking techniques, this study offers an in-depth analysis of the interaction between beta-lactoglobulin and the synthetic azo dye amaranth. This is the first of its kind to report on this subject. These results indicate that amaranth quenched the intrinsic fluorescence of BLG through a static quenching mechanism, which led to the formation of a BLG-AMA ground state complex. The study showed that AMA had a stronger binding affinity for BLG, and only one binding site was observed in fluorescence studies. The spontaneous binding process of BLG-AMA can be determined using Gibbs free energy. Additionally, the study revealed that the microenvironment around tryptophan residues changed upon interaction with AMA, as shown by the synchronous fluorescence results. The shift in the FTIR spectra revealed that amaranth caused changes in the secondary structure of the BLG. According to molecular docking studies, AMA specifically binds to BLG with more hydrogen bonds and two hydrophobic bonds; thus, the affinity of binding was stronger, and the Trp 61 residue was near the binding site of the ligand with BLG; hence, the computational results confirm the fluorescence study outcomes.

According to turbidity analysis, it was observed that at a low concentration (0.8 mM, AMA can cause amorphous aggregates on BLG at pH 2. This is due to the electrostatic and hydrophobic interactions that take place. The protein aggregates at acidic pH were found to be amorphous, as confirmed by FESEM. These findings are helpful for understanding the molecular mechanisms underlying disease-associated amyloid genesis. These results shed light on the mechanism of AMA-BLG binding interaction, which leads to protein aggregation. In vivo, AMA-induced protein modifications may have significant implications for human health and disease and could be an area of interest for future research.

6 Data availability

The authors confirm that all behavioral data to support the findings of our study are available in the paper.

References

1) Dey S, Nagababu BH. Applications of food color and bio-preservatives in the food and its effect on the human health. *Food Chemistry Advances*. 2022;1:1–13. Available from: https://doi.org/10.1016/j.focha.2022.100019.

2) Alsantali RI, Raja QA, Alzahrani AYA, Sadiq A, Naeem N, Mughal EU, et al. Miscellaneous azo dyes: a comprehensive review on recent advancements in biological and industrial applications. *Dyes and Pigments*. 2022;199:110050. Available from: https://doi.org/10.1016/j.dyepig.2021.110050.

3) Silva MM, Reboredo FH, Lidon FC. Food Colour Additives: A Synoptical Overview on Their Chemical Properties, Applications in Food Products, and Health Side Effects. *Foods*. 2022;11(3):1–32. Available from: https://doi.org/10.3390/foods11030379.

4) Awuchi CG. Whey Protein from Milk as a Source of Nutraceuticals. In: Egbuna C, Sawicka B, Khan J, editors. Food and agricultural byproducts as important source of valuable nutraceuticals. Springer, Cham. 2022;p. 159–183. Available from: https://doi.org/10.1007/978-3-030-98760-2_12.

5) Al-Shabib NA, Khan JM, Malik A, Alsenaidy AM, Alsenaidy MA, Husain FM, et al. Negatively charged food additive dye "Allura Red" rapidly induces SDS-soluble amyloid fibril in beta-lactoglobulin protein. *International Journal of Biological Macromolecules*. 2018;107(Part B):1706–1716. Available from: https://doi.org/10.1016/j.ijbiomac.2017.10.032.

6) Alresaini S, Malik A, Alonazi M, Alhomida A, Khan JM. SDS induces amorphous, amyloid-fibril, and alpha-helical structures in the myoglobin in a concentration-dependent manner. *International Journal of Biological Macromolecules*. 2023;231:123237. Available from: https://doi.org/10.1016/j.ijbiomac.2023.123237.

7) Warsi MS, Habib S, Talha M, Mir AR, Alam K, Ali A, et al. Characterization of human serum albumin modified by hair dye component, 4-chloro-1,2-phenylenediamine: Role in protein aggregation, redox biology and cytotoxicity. *Journal of Molecular Liquids*. 2021;331:115731. Available from: https://doi.org/10.1016/j.molliq.2021.115731.

8) Khan MS, Bhatt S, Tabrez S, Rehman MT, Alokail MS, Alajmi MF. Quinoline yellow (food additive) induced conformational changes in lysozyme: a spectroscopic, docking and simulation studies of dye-protein interactions. *Preparative Biochemistry & Biotechnology*. 2020;50(7):673–681. Available from: https://doi.org/10.1080/10826068.2020.1725774.

9) Khan JM, Malik A, Husain FM, Hakeem MJ, Alhomida AS. Sunset Yellow Dye Induces Amorphous Aggregation in β-Lactoglobulin at Acidic pH: A Multi-Techniques Approach. *Polymers*. 2022;14(3):1–13. Available from: https://doi.org/10.3390/polym14030395.

10) Chaves OA, Loureiro RJ, Costa-Tuna A, Almeida ZL, Pina J, Brito RM, et al. Interaction of Two Commercial Azobenzene Food Dyes, Amaranth and New Coccine, with Human Serum Albumin: Biophysical Characterization. *ACS Food Science & Technology*. 2023;3:955–968. Available from: https://doi.org/10.1021/acsfoodscitech.3c00125.

11) Wei Y, Vriesekoop F, Yuan Q, Liang H. β-Lactoglobulin as a Nanotransporter for Glabridin: Exploring the Binding Properties and Bioactivity Influences. *ACS Omega*. 2018;3(9):12246–12252. Available from: https://doi.org/10.1021/acsomega.8b01576.

12) Li M, Zhou D, Wu D, Hu X, Hu J, Geng F, et al. Comparative analysis of the interaction between alpha-lactalbumin and two edible azo colorants equipped with different sulfonyl group numbers. *Food Chemistry*. 2023;416:135826. Available from: https://doi.org/10.1016/j.foodchem.2023.135826.

13) Chen Y, Li M, Kong J, Liu J, Zhang Q. Molecular Interaction Mechanism and Preservative Effect of Lactone Sophorolipid and Lactoferrin/β-Lactoglobulin Systems. *Foods*. 2023;12(8):1–14. Available from: https://doi.org/10.3390/foods12081561.

14) Salim MM, Sharkasy MEE, Belal F, Walash M. Multi-spectroscopic and molecular docking studies for binding interaction between fluvoxamine and human serum albumin. *Spectrochimica Acta Part A: Molecular and Biomolecular Spectroscopy*. 2021;252:119495. Available from: https://doi.org/10.1016/j.saa.2021.119495.

15) Bhuin S, Halder S, Saha SK, Chakravarty M. Binding interactions and FRET between bovine serum albumin and various phenothiazine-/anthracene-based dyes: a structure–property relationship. *RSC Advances*. 2021;11(3):1679–1693. Available from: https://doi.org/10.1039/D0RA09580J.

16) Xu H, Lu Y, Zhang T, Liu K, Liu L, He Z, et al. Characterization of binding interactions of anthraquinones and bovine β-lactoglobulin. *Food Chemistry*. 2019;281:28–35. Available from: https://doi.org/10.1016/j.foodchem.2018.12.077.

17) Albani JR, Vogelaer J, Bretesche L, Kmiecik D. Tryptophan 19 residue is the origin of bovine β-lactoglobulin fluorescence. *Journal of Pharmaceutical and Biomedical Analysis*. 2014;91:144–150. Available from: https://doi.org/10.1016/j.jpba.2013.12.015.

18) El-Maksoud AAA, Cheng WA, Petersen SV, Pandiselvam RV, Guo Z. Covalent phenolic acid-grafted β-lactoglobulin conjugates: Synthesis, characterization, and evaluation of their multifunctional properties. *LWT*. 2022;172:1–10. Available from: https://doi.org/10.1016/j.lwt.2022.114215.

19) Terefe EM, Ghosh A. Molecular Docking, Validation, Dynamics Simulations, and Pharmacokinetic Prediction of Phytochemicals Isolated From <i>Croton dichogamus</i> Against the HIV-1 Reverse Transcriptase. *Bioinformatics and Biology Insights*. 2022;16:1–20. Available from: https://doi.org/10.1177/11779322221125605.

20) Elgendy EM, Al-Zahrani NA. Comparative Study of Natural and Synthetic Food Additive Dye Amaranth through Photochemical Reactions International Journal of Science and Research. *International Journal of Science and Research*. 2015;4(1):827–832. Available from: https://www.ijsr.net/archive/v4i1/SUB14713.pdf.

21) Almeida ZL, Brito RMM. Structure and Aggregation Mechanisms in Amyloids. *Molecules*. 2020;25(5):1–30. Available from: https://doi.org/10.3390/molecules25051195.

22) Al-Shabib NA, Khan JM, Malik A, Rehman MT, Alajmi MF, Husain FM, et al. Molecular interactions of food additive dye quinoline yellow (Qy) with alpha-lactalbumin: Spectroscopic and computational studies. *Journal of Molecular Liquids*. 2020;311:113215. Available from: https://doi.org/10.1016/j.molliq.2020.113215.

23) Sadat A, Joye IJ. Peak Fitting Applied to Fourier Transform Infrared and Raman Spectroscopic Analysis of Proteins. *Applied Sciences*. 2020;10(17):1–16. Available from: https://doi.org/10.3390/app10175918.

24) Fei S, Zou L, Xie X, Yang F, Chen H, Li X. Purification and Characterization of Bovine β-Lactoglobulin Variants A and B (Characterization of Bovine β-Lactoglobulin Variants). *Food Science and Technology Research*. 2020;26(3):399–409. Available from: https://doi.org/10.3136/fstr.26.399.

25) Hoppenreijs LJG, Fitzner L, Ruhmlieb T, Heyn TR, Schild K, Van Der Goot AJJ, et al. Engineering amyloid and amyloid-like morphologies of β-lactoglobulin. *Food Hydrocolloids*. 2022;124(Part A):1–15. Available from: https://doi.org/10.1016/j.foodhyd.2021.107301.